VARIABLE COEFFICIENT DISTRIBUTED PARAMETER SYSTEM MODELS FOR STRUCTURES WITH PIEZOCERAMIC ACTUATORS AND SENSORS

H.T. Banks, Y. Wang, D.J. Inman, J.C.Slater

Abstract

We consider parameter estimation problems in structures with piezoceramic actuators and sensors. The problems are discussed in the context of a variational formulation of damped second order partial differential equations with unbounded input coefficients. Approximation techniques are introduced and numerical results of parameter estimation are given. Experimental data are used to test our computational results.

I. Introduction

High fidelity dynamic models for use in identification and control algorithms are important to current efforts in understanding and design of smart material structures. A particular case of interest to us here are structures with embedded piezoceramic actuators and sensors. In addition to accurate models, which in most applications are inherently distributed in nature, computational methods (based on PDE approximation ideas) are needed. Parameter estimation techniques are of fundamental interest in model development efforts for the use of piezoceramics in such diverse areas as acoustic noise suppression and nondestructive evaluation of materials as well as the more traditional applications involving structural vibration suppression.

In this note, we report on our use of a mathematical framework (developed elsewhere – see [2, 3]) for computational methods for parameter identification in distributed parameter models for smart structures. For the class of problems we consider here (a cantilevered beam with piezoceramic patches for actuation and sensing), current models for piezoceramics lead to a system with unbounded (in usual state space formulations) input coefficients. These input coefficients, which are related to excitation of moment producing patches, involve derivatives of the delta function.

Our choice of structure is motivated by the experimental data from a beam with bonded piezoceramic sensor and actuator patches which we wish to analyze. While the structure and model are simple, we believe that they are representative in that they reveal the difficulties and possibilities inherent in developing models and methods for more complex structures containing piezoceramic materials.

We consider a cantilevered Euler-Bernoulli beam of length ℓ fixed at $x = 0$ and free at $x = \ell$. The transverse vibrations $y = y(t, x)$ are described by the system

$$\rho\frac{\partial^2 y}{\partial t^2}+\gamma\frac{\partial y}{\partial t}+\frac{\partial^2 M}{\partial x^2}=0 \qquad 0<x<\ell,\ t>0,$$
$$y(t,0)=\frac{\partial y}{\partial x}(t,0)=0, \quad M(t,\ell)=\frac{\partial M}{\partial x}(t,\ell)=0, \tag{1}$$

where ρ is the linear mass density, γ is the coefficient of viscous (air) damping and M is the internal moment. For a simple Euler-Bernoulli beam with Kelvin-Voigt or strain rate damping, the internal moment is composed of two components representing resistance to bending (with coefficient EI) and damping (with coefficient $c_D I$):

$$M(t,x)=EI\frac{\partial^2 y}{\partial x^2}(t,x)+c_D I\frac{\partial^3 y}{\partial x^2\partial t}(t,x). \tag{2}$$

If piezoelectric actuators are bonded to the beam in a configuration to produce (or sense) only bending (identically polarized patches on opposite sides of the beam excited in an out-of-phase manner – see [6, 7, 8, 10]), we have an actuator contribution $M_p(t,x)$ in the form of an input moment. For patches located between x_1 and x_2 on the beam excited by a voltage $u(t)$, this moment term has the representation

$$M_p(t,x)=K_B\{H(x-x_1)-H(x-x_2)\}\,u(t) \tag{3}$$

where H is the Heaviside or unit step at zero function and K_B is a piezoceramic material parameter depending on material properties of the beam and the patches as well as geometry. When the moment in (3) is added to that of (2) and substituted into (1), we obtain the model

$$\rho\frac{\partial^2 y}{\partial t^2}+\gamma\frac{\partial y}{\partial t}+\frac{\partial^2}{\partial x^2}\left(EI\frac{\partial^2 y}{\partial x^2}+c_D I\frac{\partial^3 y}{\partial x^2\partial t}\right)=K_B\left(\delta'(x-x_2)-\delta'(x-x_1)\right)u(t)$$
$$y(t,0)=\frac{\partial y}{\partial x}(t,0)=0, \quad M(t,\ell)=\frac{\partial M}{\partial x}(t,\ell)=0 \tag{4}$$

where δ is the Dirac delta function and $'=\frac{\partial}{\partial x}$. This is equivalent (in a sense that can be made mathematically precise – see [2, 3])
to the equation in weak or variational form

$$<\rho y_{tt}+\gamma y_t,\phi>+<EI\,y''+c_D I\,y_t''+K_B(H_1-H_2)\,u(t),\phi''>=0$$
$$y(t,0)=y'(t,0)=0, \tag{5}$$

for all $\phi\in H^2(0,\ell)$ satisfying $\phi(0)=\phi'(0)=0$. Here H_i is the shifted Heaviside function $H_i(x)=H(x-x_i)$.

The system (4) is a formal representation of the dynamics of a damped beam with piezoceramic actuators. To develop computational techniques (e.g., finite elements) based on rigorous convergence arguments, it is necessary to first have a precise formulation of this system. This can be done in the context of the equivalent system (5). One can use rather standard functional analysis techniques (the theory of sesquilinear forms and Gelfand triples—see [12]) to establish existence of unique solutions with $y(t,\cdot)\in H_L^2(0,\ell)\equiv\{\psi\in L_2(0,\ell)\mid \psi,\psi',\psi''\in L_2(0,\ell)$ with $\psi(0)=\psi'(0)=0\}$ satisfying (5) for all test functions ϕ in $H_L^2(0,\ell)$. In this sense

the initial boundary value problem in (4) is well-posed under very mild smoothness assumptions on $EI(x) > 0$ and $c_D I(x) > 0$. Detailed statements and the nontrivial arguments underlying these results can be found in [2, 3].

In this paper we will outline least squares parameter estimation problems for the systems (4) or (5), describe the experiments designed for our investigations and present numerical findings together with important conclusions that one can draw from our efforts.

II. Parameter Estimation and Approximation

The parameter estimation problems for the beam with piezoceramic actuators and sensors can be stated in terms of finding parameters which give the best fit of the parameter dependent solutions of the partial differential equations to the observation data from response of the system to various excitations. In our case, the parameters to be estimated include beam mass density $\rho(x)$, stiffness coefficient $EI(x)$ as well as damping parameters $c_D I(x)$, γ and piezoceramic material parameter K_B. Let the collection of unknown parameters be denoted by $q = (\rho(x), EI(x), c_D I(x), \gamma, K_B)$. We then can consider the least squares estimation problem of minimizing over $q \in Q$ the least squares functional

$$J(q) = \sum_i |\mathcal{C}y(t_i; q) - z_i|^2 , \tag{6}$$

where $\{z_i\}$ are given observations and $\{y(t_i; q)\}$ are the parameter dependent mild solutions of (4) or (5) evaluated at each time t_i, $i = 1, 2, \cdots, \bar{N}$. The space Q is some admissible parameter metric space while the operator $\mathcal{C}$ has two forms depending on the type of sensors. When an accelerometer is used, we minimize

$$J_a(q) = \sum_i \left| \frac{\partial^2 y}{\partial t^2}(t_i, \tilde{x}; q) - z_i \right|^2 , \tag{7}$$

where $\tilde{x}$ is the location of the accelerometer and $\{z_i\}$ are the measured accelerations. When a piezoceramic patch is used as sensor, the functional to be minimized is

$$J_p(K_s, q) = \sum_i \left| K_s \left(\frac{\partial y}{\partial x}(t_i, x_2; q) - \frac{\partial y}{\partial x}(t_i, x_1; q) \right) - z_i \right|^2 , \tag{8}$$

for the patch being located on the beam between x_1 and x_2. Here K_s is a sensor constant that also must be determined and $\{z_i\}$ are the measured voltages across the patch. Arguments to show that the voltage across the patches when used as sensors is proportional to the "accumulated strain"

$$\int_{x_1}^{x_2} \frac{\partial^2 y}{\partial x^2}(t, x) dx = \frac{\partial y}{\partial x}(t, x_2) - \frac{\partial y}{\partial x}(t, x_1) \tag{9}$$

can be found in [9].

The minimization in our parameter estimation problems involves an infinite dimensional state and an infinite dimensional (functions) admissible parameter space. Motivated by computational requirements, we thus consider Galerkin type approximations using cubic B-spline elements in the context of the variational formulation of

(5) along with piecewise constant approximations of the parameter functions. Then iterative optimization techniques are used to solve the resulting finite dimensional optimization problems. One obtains a sequence of estimates q_k of the finite dimensional optimization problems and the sequence will converge to a solution $\bar{q}$ of the original infinite dimensional problem. For a rigorous proof, see [3, 4]. In those presentations we summarize the theoretical results related to well-posedness of the infinite dimensional and approximate estimation problems, convergence of approximate parameter estimates to a solution of the original least squares estimation problem and continuous dependence of these estimates on the observation data.

In actuality, the computations for the optimization problems for (7) and (8) (and the associated functionals for the approximate systems) are best carried out after the time domain functionals have been converted to frequency domain equivalents. For example, in place of (7) one minimizes

$$\tilde{J} = \sum_l \left\{ \left| f_y^l(q) - f_d^l \right|^2 + \left| \left| U^l(q) \right| - \left| Z^l \right| \right|^2 \right\} \tag{10}$$

where $f_y^l(q)$, f_d^l are the frequencies associated with $\left\{ \frac{\partial^2 y}{\partial t^2}(t_i, \tilde{x}; q) \right\}$, $\{z_i\}$, respectively and $U^l(q)$, Z^l are the Fourier coefficients of those quantities. One can also give a convergence theory for these formulations. For complete details on implementation of these ideas as well as theoretical arguments, one can consult [5, 11].

III. Experimental Procedures

To test the above described estimation procedures a series of experiments were carried out at the Mechanical Systems Laboratory, State University of New York at Buffalo. A cantilevered aluminum beam with two attached piezoceramic patches was used as the test structure. The patches were bonded to a aluminum beam on the opposite sides of the beam at the same position. In the following two tables, the subscripts indicate the materials: b for beam and p for piezoceramic. Let ℓ be length, w be width and t be thickness; then directly measured dimension and the book values of the characteristics (stiffness and mass density) for a 2024-T4 aluminum beam are:

Table 1: Experimental beam dimensions and its characteristics.

ℓ_b (cm)	w_b (cm)	t_b (cm)	E_b (N/cm^2)	ρ_b (g/cm)
45.73	2.03	0.16	7.3×10^6	0.89

For a Piezoelectic Products model G-1195 PZT ceramic, the book values of the characteristics and the dimensions of the patch are:

Table 2: PZT ceramic patch dimensions and its characteristics.

ℓ_p (cm)	w_p (cm)	t_p (cm)	E_p (N/cm^2)	ρ_p (g/cm)
6.37	2.03	0.0254	6.3×10^6	0.78

In the tables, E is the Young's modulus and ρ is the mass density per unit length.

The beam was clamped at $x = 0$. The center of the piezoceramic was placed at 5.72 cm away from the clamped end. One 0.64 cm wide and 0.0076 cm thick copper foil to act as conducting media was glued on the beam under each piezoceramic patch. The time response data and input signal from the experimental beam were obtained using the Tektronix Analyzer 2600.

In the first example, labeled B1TAPIH, the piezoceramic patches were used as a sensor; that is, the voltage across the patch due to the beam vibration was used. The beam was excited by an impulse force applied (via an impulse hammer) on the beam along its axis at 2.54 cm away from the clamped end. The input signal was recorded from the transducer hammer (the actuator).

The Tektronix Analyzer was set so that frequencies below 64 Hz could be recorded. Two modes were observed in the response, at 6.625 Hz and 38.375 Hz, respectively.

Since the piezoceramic patches were not used as an actuator, the input voltage to the patches was zero. Hence the term

$$K_B \Big(\delta'(x - x_2) - \delta'(x - x_1) \Big) u(t)$$

in equation (1.4) is zero. Instead, a term $f(t, x)$ which represents the hammer input is introduced on the right hand side of the partial differential equation in (1.4). The functional J_p in equation (2.3) was minimized. In this example, K_B was not involved, therefore was not identifiable. The parameter vector to be identified was $q = (EI(x), \rho(x), c_D I(x), \gamma, K_s)$. The mass density, stiffness and Kelvin-Voigt damping coefficients are functions of position along the beam. To agree with geometry of the structure, we assumed that they are piecewise constant functions as shown in Figure 1.

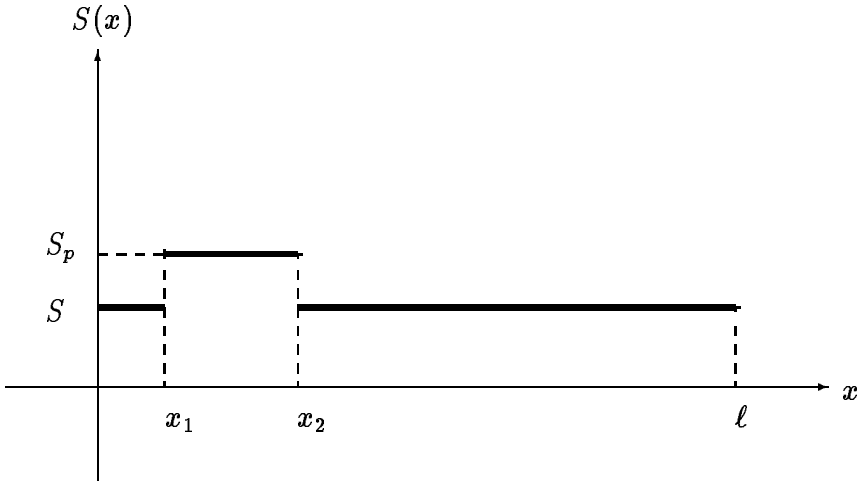

Figure 1: $\rho(x)$, $EI(x)$, $c_D I(x)$ function shape $S(x)$.

In the second example, labeled B1TAOIV, the piezoceramic patches were used as the actuator and an accelerometer as the sensor. The accelerometer weighing 0.5 gram was located at $x = 2.14$ cm. Our choice of the location of the accelerometer was to made so as to minimize the dynamical effects of the accelerometer (e.g. effects due to the weight of the accelerometer and the vibration of the wire attached to it). A narrow triangle (approximating an impulse) voltage was applied to the patches to excite the beam. The ceramic patches were excited out of phase so as to produce input moments as modeled in (3) or (4) above. In order to maintain a constant E_p through out the data acquisition period following excitation when only accelerometer data was collected (i.e. the ceramic patch was not used as a sensor), a zero voltage supply (not zero current) to the patches was provided. In this case, the parameter vector was $q = (EI(x), \rho(x), c_D I(x), \gamma, K_B)$.

In the first example, we began the parameter identification by holding damping related parameters fixed while identifying parameters $EI(x)$ and $\rho(x)$ to first obtain a frequencies match. We used measured values together with book values as our initial guess. The initial value for the constant in the part of beam without the patches is a straight forward calculation with the values given in Table 1, $EI = 0.495$ and $\rho = 0.089$. For the constant for the segment containing the patches, we simply superposed characteristics of the beam and the patches (we ignored the glue and copper foil) and obtained $EI = 1.0$ and $\rho = 0.168$. Then the estimation was carried out on the damping parameters $c_D I$ and γ, and piezoceramic related parameter K_s, while keeping the parameters $EI(x)$ and $\rho(x)$ at the optimal values obtained. The initial values were $c_D I(x) = 0.825 \times 10^{-5}$ and $\gamma = 0.00183$. The optimal values obtained from the first example were used as initial values in the second example. Since both examples are from the same structure with different sensors and actuators, we anticipated that the estimated parameters from the two examples might be close.

A summary of the estimation results is given in Table 3. For comparison, results from both examples are listed in the same table. The measured and handbook quantities (when available) are also listed in the table as "given" values.

Table 3: Given and estimated structural parameters

		given	B1TAPIH	B1TAOIV
EI ($\mathrm{N{\cdot}m^2}$)	beam	0.495	0.491	0.505
	beam + PZT	—	0.793	0.798
ρ (kg/m)	beam	0.089	0.093	0.096
	beam + PZT	0.168	0.433	0.441
$c_D I$	beam		0.649×10^{-5}	0.637×10^{-5}
	beam +	—	1.255×10^{-5}	1.275×10^{-5}
γ		—	0.013	0.013
$\tilde{K}_s$		—	4682.342	—
K_B		—	—	1.870

The results (graphs) are reported in the order described above. The example B1TAPIH is given in Figure 2 and the example B1TAOIV is shown in Figure 3. In each figure, there are four parts: part (a) is the recorded experimental data, (b) is the model response with the estimated parameters given in Table 3, (c) is the amplitude of the FFT of the experimental data (in solid lines) and model response (in dashed lines), and in part (d), both experimental data (in solid lines) and the model response (in dashed lines) are presented on a shorter time interval in one plot to exhibit the details of how well the model fits the experimental data.